communications earth & environment

ARTICLE

https://doi.org/10.1038/s43247-023-00726-4 OPEN

Preclassic environmental degradation of Lake Petén Itzá, Guatemala, by the early Maya of Nixtun-Ch'ich'

Brooke A. Birkett [1], Jonathan Obrist-Farner [1✉], Prudence M. Rice[2], Wesley G. Parker[3], Peter M. J. Douglas[3], Melissa A. Berke[4], Audrey K. Taylor [4], Jason H. Curtis[5] & Benjamin Keenan [3]

Paleolimnological evidence indicates the ancient Maya transformed terrestrial ecosystems by felling forest vegetation to construct large civic-ceremonial centers and to expand agriculture. Human settlements influenced lacustrine environments but the effects of Maya activities on aquatic ecosystems remain poorly studied. Here we analyzed a sediment core from Lake Petén Itzá, Guatemala, to infer paleoenvironmental changes resulting from Maya occupation of the archaeological site of Nixtun-Ch'ich'. Increases in charcoal and fecal stanol concentrations indicate Maya occupation of the Candelaria Peninsula by the late Early Preclassic period. Geochemical proxies reveal a period of lake ecosystem alteration during construction and expansion of the city's urban grid in the Middle and Late Preclassic periods. Depopulation of the city in the Terminal Preclassic resulted in a decline in lake trophic state. Whereas previous studies of Petén waterbodies have indicated depressed lacustrine primary production, the core collected near Nixtun-Ch'ich' shows evidence of ancient Maya lake ecosystem deterioration.

[1] Geosciences and Geological and Petroleum Engineering Department, Missouri University of Science and Technology, Rolla, MO 65409, USA. [2] Department of Anthropology (emerita), Southern Illinois University Carbondale, Carbondale, IL 62901, USA. [3] Department of Earth and Planetary Sciences and Geotop Research Center, McGill University, Montreal, QC H3A 0E8, Canada. [4] Civil and Environmental Engineering and Earth Sciences Department, University of Notre Dame, Notre Dame, IN 46556, USA. [5] Department of Geological Sciences, University of Florida, Gainesville, FL 32611, USA. ✉email: obristj@mst.edu

Paleolimnological studies have documented the impacts of ancient Maya activities on the lowland terrestrial environments of eastern Mexico, Guatemala, and Belize, specifically through widespread deforestation for urbanization and agricultural development[1–8]. Land clearance led to rapid soil erosion and siltation of waterbodies, recorded as thick deposits of inorganic colluvium, sometimes referred to as "Maya clay" that accumulated during the Preclassic (ca. 900 cal yr BCE–200 CE; hereafter BCE, CE) and Classic (200–950 CE) Maya archaeological periods[1,6,7,9,10]. Ancient Maya occupation was also linked to periods of high fire frequency, likely related to the early use of slash-and-burn (swidden) agricultural techniques[11]. The prominence of large-scale ancient Maya land alterations during the Preclassic and Classic periods has also led some researchers to propose a regional "Early Anthropocene", or "Mayacene", ca. 1000 BCE–1000 CE[12–14]. However, these studies primarily focus on evidence for vast human-mediated land transformations and have overlooked lacustrine ecosystem responses to anthropogenic disturbances during those times.

Widespread land-cover change might be expected to have influenced the trophic status and aquatic ecosystems of local lakes through enhanced nutrient loading and consequent shifts in aquatic community composition. Despite the presence of archeologically documented, dense Maya populations around the lakes in the central Department of Petén, northern Guatemala[15], paleolimnological studies have so far failed to reveal evidence of large-scale lake ecosystem alterations as a result of Maya activities. It has been suggested that intense siltation of waterbodies, as a result of land clearance, limited light penetration, and adsorbed dissolved nutrients, thereby suppressing lacustrine primary production[16,17]. However, given evidence for recent trophic state increase and high aquatic macrophyte diversity and abundance in Guatemalan lakes associated with rapid population growth in the 20th century (e.g., Lake Petén Itzá[18–20] and Lake Izabal[21]), it seems likely that the establishment of ancient Maya urban centers near waterbodies would have also influenced lake ecological status, as has been observed in the Maya highlands[22]. Despite this disparity between observed, modern lake ecosystem changes and previous inferences of changes during lowland Maya occupation of the watershed, there are no multi-proxy sediment core datasets investigating this issue.

Here, we conduct an extensive, multi-proxy paleolimnological investigation on a radiocarbon-dated sediment core from Lake Petén Itzá, Guatemala. The core was collected from the western arm of the lake, adjacent to a southern lowland Maya archeological site on the Candelaria Peninsula called Nixtun-Ch'ich' (Fig. 1). Stratigraphic fluctuations in several organic matter geochemical proxies reveal a previously undocumented period of aquatic ecosystem alteration during times of Maya occupation at Nixtun-Ch'ich', providing further evidence of anthropogenic environmental impacts in the Maya Lowlands. The onset of aquatic ecosystem changes coincides with the early Maya occupation at the site and changes in land-use practices, suggesting that prolonged and spatially concentrated ancient human activities had a profound impact on this shallow arm of the lake. Whereas massive Maya-induced siltation in other Petén lakes may have suppressed lake productivity, paving of the riparian gridded city of Nixtun-Ch'ich'[23–25] likely enhanced nutrient-laden runoff from the urban center, which fueled primary productivity in the relatively shallow and hydrologically isolated southern basin of Lake Petén Itzá. A sharp decrease in lithogenic elements at the top of the disturbance zone in core PI-NC-1 indicates an abrupt reduction or cessation of human constructional activities at the end of the Late Preclassic period[8], and the lake ecosystem experienced a relatively swift, but incomplete, recovery after partial depopulation of the city during the Terminal Preclassic. The sediment record from Lake Petén Itzá enabled us to investigate the causes and timing of lake ecosystem change during the ancient Maya occupation and explore the lake's response to changing human-mediated catchment conditions over decadal to centennial time scales.

Results

Study site. Lake Petén Itzá is the largest (~100 km^2) and deepest (165 m) of eight closed-basin waterbodies in the central Petén lakes region of northern Guatemala (Fig. 1). The lake occupies two connected basins that formed in karst depressions in marine limestones of Late Cretaceous to Tertiary and Paleocene-Eocene age[26,27]. The lake's larger, deeper northern basin is bounded on the north shore by the steep wall of an east-west normal fault[26,28], and the southern basin has a gently sloping bathymetry, with water depths of less than 20 m[29].

The 515-cm-long sediment core (PI-NC-1) was collected in July 2018, in 8.4 m of water ~200 m south (16°56'36" N, 89°55'56" W) of the early Maya archeological site of Nixtun-Ch'ich', in the narrow, western arm (7 km long × 250–450 m wide) of the lake's southern basin (Fig. 1). Nixtun-Ch'ich' contains an urban core that covers 1.1 km^2 and is centered by an *axis urbis*[23]. The city also features a unique, modular, urban gridded layout consisting of seven north-south "avenues" that intersect with six east-west "streets", covering an area of 2.5 km^2[30,2,25]. This system of roughly orthogonal corridors, supplemented with canals in areas that likely experienced intense runoff during rainfall events, facilitated drainage from the site[24]. The sediment core site lies downstream and bathymetrically downgradient from two of the archeological site's major north-south trending avenues (G and H), which run adjacent to major structures in Nixtun-Ch'ich' and likely served as focal points for the delivery of dissolved and suspended material in runoff to this arm of the lake (Fig. 1).

Nixtun-Ch'ich' was a long-lived civic-ceremonial center first occupied in the late or terminal Early Preclassic period (pre-900/800 BCE), as determined from scattered, small pottery fragments[31]. Stratified occupation and construction began in the Middle Preclassic period (ca. 900/800–500/400 BCE) and was sustained through the Late Preclassic. Archeological excavations date the initial emplacement of the site's atypical urban grid to the heavily occupied Middle Preclassic period (ca. 800–500 BCE), when it was a primate city (i.e., at the top tier of a primate settlement system[23,25,30]). Primate cities typically have a disproportionately larger size (spatially and demographically) and greater functional centralization than nearby secondary centers/satellites (e.g., in this case, Tayasal, T'up, and Sacpuy 1[23]). The substantial construction of Nixtun-Ch'ich' continued into the Late Preclassic period[31] and ended around 100 CE. Cessation of building and/or partial depopulation of the site[8] coincides with a proposed "Late Preclassic collapse" that has been identified at other southern Maya lowland centers[32]. Afterward, occupation of the site persisted through the Classic and Postclassic periods, and beyond the Spanish conquest (1697 CE[33]) into Colonial times[31,34].

Modern human and livestock disturbance in the Lake Petén Itzá catchment has been associated with increased trophic state[18,19] and aquatic weed species (e.g., *Eleocharis interstincta, Najas guadalupensis, Vallisneria americana, Potamogeton illinoensis,* and *Eichornia crassipes*), especially near wastewater and sewage discharges with elevated nutrient loading[20]. These aquatic weeds tolerate extreme conditions of disturbance and are widely distributed in the waterbody[20]. Lake Petén Itzá has high aquatic plant biodiversity, with 28 identified species of aquatic plants (9 submergent, 13 emergent, and 6 floating[20]), including both native species (e.g., *Typha domingensis* and *Cladium jamaicensis*) and introduced aquatic weed species (e.g., *Eichornia crassipes* and

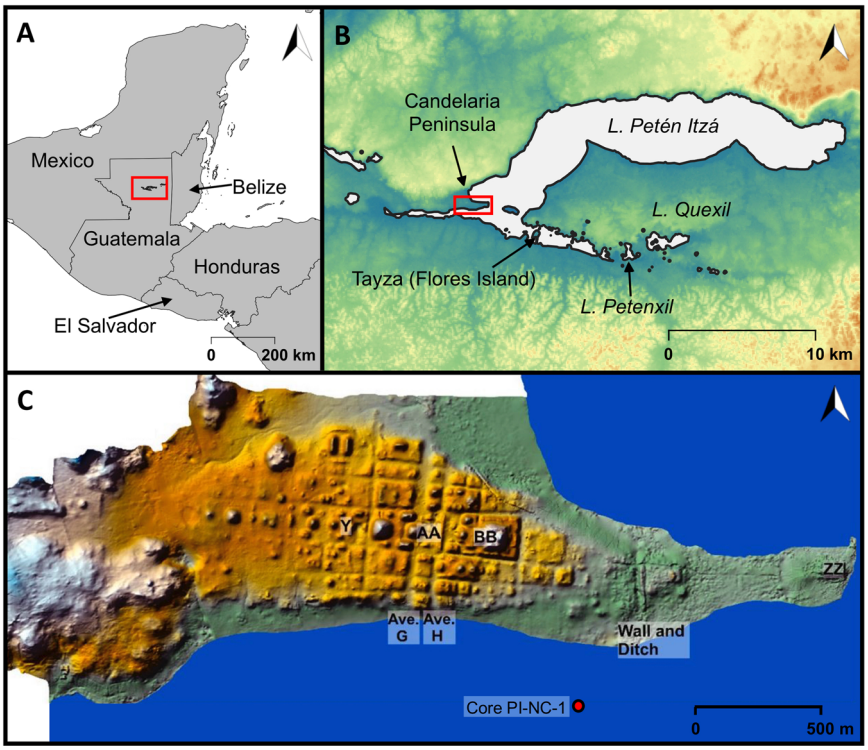

Fig. 1 Maps of Central America and Lake Petén Itzá. A Map of the Yucatán Peninsula region in Central America, with the location of the central Petén lakes region indicated by the small, red rectangle in northern Guatemala. **B** Map of Lake Petén Itzá, showing the location of the Candelaria Peninsula at the western end of the lake, which hosts the archeological site of Nixtun-Ch'ich'. **C** Map of Nixtun-Ch'ich', showing the city's unique gridded layout and the site where the lake sediment core was collected (modified from Rice and Pugh[23]).

Pistia stratiotes) that provide wildlife refuge, help stabilize nutrient discharges, and prevent waterbody deterioration[20].

Core chronology. We modified the age-depth model of sediment core PI-NC-1 used by Obrist-Farner and Rice[8] by including six additional radiocarbon dates (Supplementary Data 1 and Figs. S1, S2). The Bayesian radiocarbon age-depth model (Methods) suggests that the 515-cm core captures the last ~7000 years. We subdivided the core into four sediment zones based on physical characteristics of the sediment (color, texture, grain size). Here, we present data from 313 to 58 cm core depth from the first three zones of the core. Considering the uncertainties associated with our age-depth model, these three zones span the interval from ca. 2050 BCE (95% range 2255–1870 BCE) to 1490 CE (95% range 1365–1610 CE), with the largest uncertainty associated with the middle of Zone 2 (mean uncertainty of ± 300 years) where datable material in the core was absent. First, we present data from the upper portion of Zone 1, spanning from ca. 2050 to 710 BCE (95% range 890–470 BCE), which consists of gray, thickly laminated to very thinly bedded, carbonate-rich silty clays with variable amounts of gastropod shells (Figs. 2, 3). Then, we specifically focus on the interval between 209 cm (710 BCE) and 164 cm (280 CE; 95% range 45 BCE–560 CE), which exhibits distinctive sediment characteristics. This interval of sediment (Zone 2) changes to a dark brown-gray, massive, carbonate-rich clay with very sparse organic debris and gastropod shell fragments (Figs. 2, 3). Zone 2 is coeval with the "Maya clay" unit observed in sediment cores from several lakes across the southern Maya lowlands[1,6,9]. Zone 3 spans from ca. 280 CE to 1490 CE (95% range 1360–1610 CE) and consists of light brown, very thinly bedded, organic and carbonate-rich silty clays with variable amounts of gastropod shell fragments (Figs. 2, 3).

Zone 1 (2050–710 BCE). Geochemical data in Zone 1 exhibit relatively constant values from about 2050 to 710 BCE, representing fairly stable, pre-disturbance lake conditions prior to substantial anthropogenic activity near the core location. Total organic carbon (TOC) and total nitrogen (TN) remained relatively constant, with average values of 2.8 ± 0.6 wt% and 0.2 ± 0.03 wt%, respectively (Fig. 2). Total *n*-alkane (saturated hydrocarbon) abundance, which reflects a fraction of the organic matter (OM) from vascular plant leaf waxes, was relatively constant and averaged 1.8 ± 0.4 µg/g (Fig. 2). TOC/TN mass ratios (i.e., C/N ratios) were also relatively constant and averaged 13.5 ± 1.1 (Fig. 2), suggesting mixed input of OM from both lacustrine algae and terrestrial and aquatic plants[35,36] (Fig. S3 and Supplementary Data 2). Nitrogen and carbon stable isotope values of bulk organic matter ($\delta^{15}N_{org}$ and $\delta^{13}C_{org}$) had average values of 2.7 ± 0.4‰ and −25.0 ± 0.7‰, respectively (Fig. 2). The mean carbon stable isotope value indicates that sediment OM was derived primarily from lake algae and C_3 land and aquatic plants[35,36] (Fig. S3). Compound-specific $\delta^{13}C$ of *n*-alkanes averaged −27.5 ± 0.2‰, −30.0 ± 0.6‰, −29.6 ± 0.8‰, −30.2 ± 0.7‰, −30.0 ± 1.0‰, −29.1 ± 1.0‰, and −28.8 ± 0.8‰ for C_{23}, C_{25}, C_{27}, C_{29}, C_{31}, C_{33}, and C_{35}, respectively (Fig. 2). These values imply that deposited mid- to long-chain *n*-alkanes were primarily derived from C_3 plant waxes[35,36].

At the bottom of Zone 1, from about 2050 to 1070 BCE, charcoal averages 359 ± 80 particles/cm^3 (Fig. 3), likely representing the occurrence of both natural and anthropogenic fires in the area. At the top of Zone 1 (~1070 to ~710 BCE), charcoal increases abruptly, averaging 573 ± 308 particles/cm^3 (Fig. 3). Charcoal reached a maximum of 1,476 particles/cm^3 at ~1070 BCE (95% range 1220–945 BCE), with another increase to 1062 particles/cm^3 at ~890 BCE (95% range 990–815 BCE). Higher-than-average charcoal abundances from ~1070 to ~710 BCE

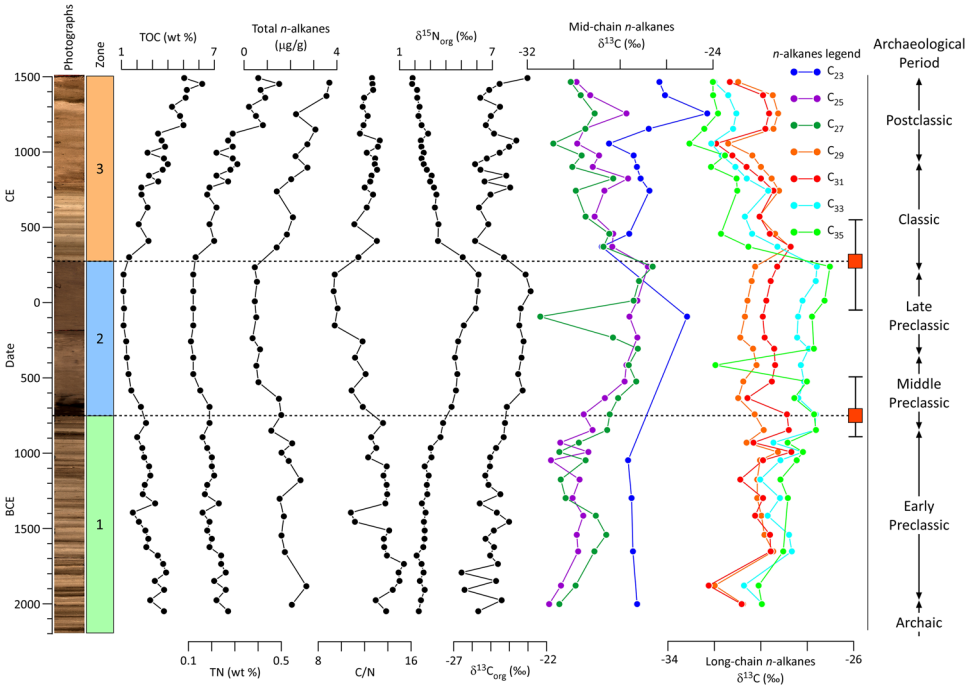

Fig. 2 Organic geochemical proxies from core PI-NC-1. Total organic carbon, total nitrogen, total *n*-alkane abundance, C/N mass ratio, nitrogen and carbon stable isotopes of bulk organic matter, and compound-specific carbon stable isotopes for mid- and long-chain *n*-alkanes plotted against time and the corresponding archeological periods. Date uncertainties from our age-depth model at the boundaries of Zone 2 (black dashed lines) are shown with box and whisker plots, in which the weighted means are represented by red boxes and the 95% ranges by whiskers.

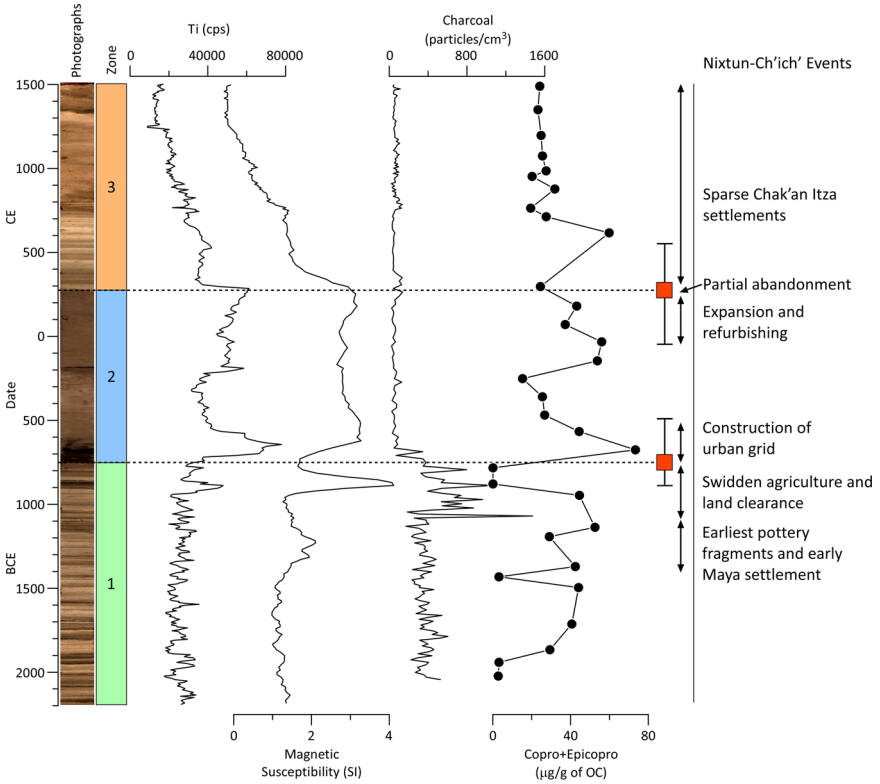

Fig. 3 Inorganic proxies, charcoal, and fecal stanol concentrations from core PI-NC-1. Titanium abundance (expressed in counts per second [cps]), magnetic susceptibility (expressed in the international system of units [SI]), charcoal abundance, and coprostanol + epicoprostanol plotted against time and events in Nixtun-Ch'ich'. Coprostanol + epicoprostanol concentrations are normalized to TOC. Date uncertainties from our age-depth model at the boundaries of Zone 2 (black dashed lines) are shown with box and whisker plots, in which the weighted means are represented by red boxes and the 95% ranges by whiskers.

indicate high local fire activity, likely reflecting slash-and-burn agricultural practices and fire clearance of the Candelaria Peninsula by the early Maya prior to the construction of Nixtun-Ch'ich'.

Fecal stanol/sterol concentrations (Fig. 3), expressed as μg per gram (g) of organic carbon (OC), remained consistently low for the first ~3000–3750 years of the sediment record, and likely represent the natural (background/wildlife) fecal material input to the lake (Supplementary Data 3). We focus our analysis primarily on coprostanol + epicoprostanol (copro+epicopro), as this is the fecal stanol that is most diagnostic of human populations[37,38], and is correlated with a catchment population in modern lake sediments from the Maya Lowlands[39]. Cholesterol, cholestanol, and stigmastanol provide supporting data for our analysis (Supplementary Notes and Fig. S4). Copro + epicopro values were highly variable, averaging 25.8 ± 17.5 μg/g of OC before ~1900 BCE (Fig. 3 and Supplementary Data 3), with a slightly higher average of 28.5 ± 20.2 μg/g of OC after ~1900 BCE in Zone 1. Fluctuations in these organic molecules after ~1900 BCE probably indicate early, sparse human settlement of the area that later became the urban center of Nixtun-Ch'ich'. Our results are similar to those by ref. [39] that show, for example, human presence in the catchment of Laguna Itzán preceding archeological evidence for permanent settlements in the area.

Zone 2 (710 BCE–280 CE). Zone 2 displays distinct changes in all geochemical variables. Both TOC and TN decreased, averaging 1.4 ± 0.4 wt% and 0.1 ± 0.03 wt%, respectively (Fig. 2). These values are about half of those in Zone 1, indicating either lower primary productivity from reduced nutrient availability[40] or dilution of organic matter by enhanced clastic sedimentation[2,41,42]. Total *n*-alkane abundance followed the trend observed in TOC and was relatively low, averaging 0.6 ± 0.3 μg/g (Fig. 2), likely as a result of organic matter dilution within the Maya clay unit. C/N ratios decreased gradually until reaching a relatively constant value of 9.5 ± 0.1 from ca. 150 BCE to 200 CE (Fig. 2), suggesting a greater relative contribution to sediment OM from lacustrine algae[35] (Fig. S3), aquatic macrophytes[36,43,44], and/or nitrogen-rich soil OM[45,46]. At the same time, $\delta^{15}N_{org}$ and $\delta^{13}C_{org}$ values gradually increased until reaching highs of 6.0 ± 0.1 and −23.1 ± 0.3‰, respectively, which persisted from ca. 100 BCE to 200 CE (Fig. 2), indicating enhanced lacustrine primary productivity[35,45,47] and aquatic macrophyte abundance[48]. *n*-Alkane $\delta^{13}C$ for C_{23}, C_{25}, C_{27}, C_{33}, and C_{35} gradually increased (similar to $\delta^{13}C_{org}$) to highs of −25.1‰, −26.8‰, −26.6‰, −27.6‰, and −27.0‰ ca. 200 CE, respectively (Fig. 2), presumably reflecting isotopic changes in shallow-water aquatic vegetation as a result of changes in paleoproductivity[43,44]. $\delta^{13}C$ of *n*-alkanes C_{29} and C_{31} remained relatively constant and varied less than that of other *n*-alkane homologs, averaging −30.5 ± 0.3‰ and −29.7 ± 0.4‰, respectively (Fig. 2), implying a dominantly terrestrial source[49,50]. Charcoal concentration was also low, averaging 62 ± 49 particles/cm^3 (Fig. 3), probably resulting from reduced fire frequency following earlier land clearance and urbanization of the peninsula. Although highly variable, copro +epicopro values were elevated overall in Zone 2, averaging 41.6 ± 17.9 μg/g of OC (Fig. 3), pointing to generally increased and sustained human fecal runoff to the lake relative to Zone 1. The observed changes in lake conditions are coeval with heavy urban construction and dense occupation at Nixtun-Ch'ich'[8,23,31], suggesting that soil disturbance from construction and earlier agriculture, coupled with nutrient-laden urban runoff, accelerated delivery of sediment and nutrients that contributed to the gradual deterioration of the water quality in the shallow, western arm of Lake Petén Itzá from about 710 BCE to 280 CE.

Zone 3 (280–1490 CE). The transition from Zone 2 to Zone 3 is characterized by rapid changes in all geochemical variables. Throughout Zone 3, TOC and TN increased gradually, with average values of 3.6 ± 1.2 wt% and 0.3 ± 0.1 wt%, respectively (Fig. 2). Total *n*-alkane abundance also rose, following the trend of TOC, averaging 2.4 ± 0.7 μg/g (Fig. 2). C/N ratios were higher than in Zone 2 and maintained a relatively constant average of 12.4 ± 0.6 (Fig. 2), suggesting sediment OM was composed of a mixture of lake algae and aquatic and land plants[35,36,43] (Fig. S3). Stable isotope values shifted to more negative values, with $\delta^{15}N_{org}$ and $\delta^{13}C_{org}$ averaging 2.8 ± 0.7‰ and −24.9 ± 0.7‰, respectively (Fig. 2). *n*-Alkane $\delta^{13}C$ for C_{23}, C_{25}, C_{27}, C_{33}, and C_{35} also became more isotopically depleted (similar to $\delta^{13}C_{org}$), averaging −27.0 ± 1.2‰, −28.9 ± 0.7‰, −29.5 ± 0.7‰, −30.9 ± 0.9‰, and −31.8 ± 0.7‰, respectively (Fig. 2). *n*-Alkane $\delta^{13}C$ for C_{29} and C_{31}, however, averaged −29.8 ± 0.8‰ and −30.2 ± 0.9‰, respectively, comparable to values observed in Zone 2 (Fig. 2). Charcoal concentrations in Zone 3 remained low and resembled those in Zone 2, averaging 63 ± 24 particles/cm^3 (Fig. 3), indicating continued low local fire activity after construction of the city. Lower human fecal contamination is supported by low copro +epicopro values in Zone 3, averaging 28.0 ± 11.1 μg/g of OC, commensurate with the average observed in Zone 1 after ~1900 BCE (Fig. 3). Variations in these organic molecules after ~280 CE suggest reduced human population in the area, supporting archeological evidence of sparse Maya settlement in the Candelaria Peninsula after the Terminal Preclassic.

Discussion

Our data highlight a period of substantial human-induced disturbance in southwestern Lake Petén Itzá between ca. 710 BCE and 280 CE. Archeological findings suggest considerable population growth at Nixtun-Ch'ich' during the Middle Preclassic (900/800–400/300 BCE[31]), coincident with our paleolimnological evidence of deteriorating environmental conditions in the western arm of the lake. We infer relatively pristine (oligotrophic) and stable lake and environmental conditions in the older part of our sediment record, prior to the period of archeologically documented human disturbance. Only minor changes in the lake ecosystem were detected near the end of the Early Preclassic, when early Maya land cover changes began ca. 1100 BCE, several hundred years before the establishment of the site's urban grid from about 800 to 500 BCE[8,25,30]. Increasing charcoal abundance from ca. 1070 to 710 BCE records a greater number of fire events in the catchment of the western arm of the lake and marks the earliest human-mediated burning at this location, suggesting the ancient Maya farmers were well-established on the Candelaria Peninsula and in surrounding areas by the end of the Early Preclassic. Temporal coincidence of increased charcoal abundance in core PI-NC-1 (Fig. 3) with the first appearance of corn (*Zea mays*) pollen in the northern basin of Lake Petén Itzá (~1050 BCE[10]) points to the early use of swidden agricultural practices by Maya populations around the lake, and perhaps by the early Maya who constructed platform ZZ1 at the eastern end of the Peninsula in the late Early Preclassic period (pre-1000/900 BCE[34]). Mueller et al[10]. also reported increases in pollen of disturbance taxa (*Asteraceae*, *Ambrosia*, and *Chenopodiaceae*) from about 1050 BCE to 950 CE in Lake Petén Itzá, providing supporting evidence for Maya land clearance beginning in the late Early Preclassic. Additionally, our fecal stanol data, particularly higher average copro+epicopro concentrations (Fig. 3 and S4), along with an early increase in sediment magnetic susceptibility ca. 1330 BCE (95% range 1445–1190 BCE) (Fig. 3), support an inference for early, but probably sparse, Maya settlement at the

site of Nixtun-Ch'ich' during the late Early Preclassic, beginning ca. 1400–1300 BCE. Similarly, high fecal stanol concentrations have also been reported at other early Mayan sites in the Petén lowlands prior to evidence for urban development[39].

Several distinct changes in the sediment begin ca. 710 BCE, during the urbanization of Nixtun-Ch'ich'. Sedimentological changes indicate a rapid shift in lake and catchment conditions leading to the deposition of a relatively thin Maya clay unit at this site throughout most of the Middle and Late Preclassic periods (ca. 800 BCE–200 CE). Paleolimnological studies in several smaller central Petén lakes suggested that forest clearance and urban construction led to rapid soil erosion and siltation of waterbodies, in some cases resulting in the deposition of Maya clay units that are several meters thick[1,9,17]. In the eastern arm of Lake Petén Itzá's southern basin, however, the Maya clay, which spanned approximately 1700 years, did not appear as an obvious, distinct unit and could only be identified with geochemical and magnetic susceptibility records[3], demonstrating that Maya clay deposition was heterogeneous across the Petén lakes. In our core from the western arm of the lake's southern basin, the Maya clay is ~0.5 m thick and spans only about 1000 years without a slight decrease in sediment accumulation rates (Fig. S2) after the urban grid of Nixtun-Ch'ich' was constructed. Higher Ti abundance and an increase in magnetic susceptibility beginning ca. 710 BCE (Fig. 3) likely reflect highly localized erosional signals caused by human activities at Nixtun-Ch'ich' (e.g., grid establishment and maintenance[8]), rather than more widespread changes in the lake catchment (e.g., deforestation).

The initiation of gradual increases in $\delta^{15}N_{org}$ and $\delta^{13}C_{org}$, with a simultaneous gradual decline in the C/N ratio, coincided with an abrupt increase in local fire activity ca. 1070 BCE, as inferred from the charcoal record (Figs. 2, 3). Local fires related to swidden agricultural practices likely caused pulses of soil erosion (and consequent sediment deposition in the lake) that delivered greater nutrient loads to the waterbody, thereby altering lake environmental conditions. For example, higher titanium and magnetic susceptibility values ca. 890 BCE (Fig. 3), as well as increases in several detrital elements[8] (Fig. S5 and Supplementary Data 3), correspond with charcoal evidence for large fire events that also mark the beginning of more pronounced changes in organic matter constituents (Fig. 2). By the time construction of the urban grid in Nixtun-Ch'ich' began ca. 800 BCE[23,25], rising values of both $\delta^{13}C_{org}$ and $\delta^{15}N_{org}$, accompanied by similarly increasing $\delta^{13}C$ values for mid-chain *n*-alkanes (C_{25} and C_{27}) and declining C/N ratios (Fig. 2), likely indicate greater contributions of aquatic (algal and/or macrophyte-derived) OM to the sediment[35,36,43,44,48]. These conditions were sustained through the Late Preclassic Maya occupation, suggesting intensifying cultural eutrophication and/or expansion of shallow-water macrophyte communities adjacent to Nixtun-Ch'ich' during the Middle and Late Preclassic. Synchronous carbon and nitrogen stable isotope enrichment also support an inference for lake ecosystem alteration. Initially, aquatic primary producers preferentially utilize the lighter carbon (^{12}C) and nitrogen (^{14}N) isotopes during photosynthesis and protein synthesis, respectively, but as those reservoirs are progressively depleted, algae and macrophytes are forced to incorporate the heavier isotopes (^{13}C and ^{15}N) and thus become isotopically enriched[35,43,45,47].

Short-chain (C_{17}–C_{21}) *n*-alkane abundances, which are generally produced by aquatic algae and microbes[49,51], were low in core PI-NC-1 (Fig. S6), potentially indicating low rates of primary production in the lake. However, this was also observed throughout an 85 ky sediment record in Lake Petén Itzá[52], suggesting that short-chain alkanes may not be produced in large quantities or are not well preserved in the lake. Alkane abundances are instead dominated by long-chain (C_{29}–C_{35}) *n*-alkanes (Fig. S6), generally interpreted to represent a dominant terrestrial source[49]. Moreover, several emergent macrophytes (e.g., *Eichornia crassipes, Phragmites australis*) found along the modern shoreline of Lake Petén Itzá[20] also produce large quantities of long-chain *n*-alkanes[50,53] and possibly contributed to the predominance of long-chain *n*-alkanes in core PI-NC-1 through time (Fig. S6). Several species of aquatic plants that contain high amounts of mid-chain *n*-alkanes C_{23}, C_{25}, and C_{27} (e.g., *Chara, Utricularia foliosa*[44,54]) are also present along the modern shoreline of Lake Petén Itzá[20], and likely dominated isotopic changes in mid-chain homologs observed in core PI-NC-1 (Fig. 2). Similar ^{13}C enrichment of long-chain *n*-alkanes C_{33} and C_{35} with mid-chain *n*-alkanes C_{25} and C_{27} (Fig. 2) may have also been influenced by the presence of aquatic plants dominated by both mid- and long-chain homologs, such as *Cladium jamaicense* (an aquatic sedge) and *Potamogeton* (a submerged macrophyte) in the lake[20,44,50]. Pronounced ^{13}C enrichment of mid-chain *n*-alkanes C_{25} and C_{27} (and probably long-chain *n*-alkanes C_{33} and C_{35}) during the Middle and Late Preclassic Periods supports our theory of the expansion of shallow-water macrophyte communities in the western arm of Lake Petén Itzá (i.e., expansion of aquatic weed species) resulting from enhanced inputs of clastic materials, nutrient-rich runoff, and human waste from Nixtun-Ch'ich'.

There are, however, possible alternative explanations for the stratigraphic shifts displayed by some geochemical proxies. First, an increase in compound-specific $\delta^{13}C$ and $\delta^{13}C_{org}$ can also indicate a greater relative contribution to sediment OM from C_4 (maize and other tropical grasses) versus C_3 (woody trees and shrubs) vegetation[10,55,56]. However, C/N ratios in core PI-NC-1 are inconsistent with those of C_4 vegetation (Fig. S3, Supplementary Data 2) and maize ($\delta^{13}C_{org} = -12‰$[57]), and the similarity between $\delta^{13}C_{org}$ and $\delta^{13}C$ values for mid-chain *n*-alkanes C_{25} and C_{27} (Fig. S7) suggests that the isotopic observations are mainly driven by aquatic plants (i.e., macrophytes) that produce mid-chain *n*-alkanes[35,36,43,44,48]. Notably, the lack of ^{13}C enrichment in the C_{29} and C_{31} *n*-alkanes, which are the dominant *n*-alkanes in most terrestrial plants and are present in maize (dominant *n*-alkanes are C_{25} – C_{31}, with C_{27} and C_{29} present in the highest amounts[57,58]), suggests that at this time, C_4 plants did not contribute substantially to explain the observed enrichment in $\delta^{13}C_{org}$. Additionally, changes in $\delta^{13}C_{org}$ do not correlate with initial forest decline beginning ca. 2550 BCE[10] or abrupt increases in pollen from disturbance taxa ca. 1050 BCE[10] or charcoal ca. 1070 BCE, which likely reflect early maize cultivation practices in the vicinity of Lake Petén Itzá. This hints that the observed gradual enrichment in $\delta^{13}C_{org}$ is not driven by vegetation changes in the catchment. Second, given an inferred reduction of terrestrial riparian vegetation in the catchment after ca. 710 BCE, reduced terrestrial OM input to the lake could have augmented the relative proportion of lacustrine OM in sediments, even with constant lacustrine and aquatic macrophyte primary productivity, yielding a false eutrophication signal. However, if this were the case, shifts in OM proxies would likely persist through the Classic Period until forest recovery ca. 900–1200 CE[2,59]. Third, enhanced fecal input could also cause a rise in $\delta^{15}N_{org}$[35,45], corresponding with greater average copro+epicopro content in the lake sediments, although human fecal inputs also occurred in Zone 1 with no observed changes in $\delta^{15}N_{org}$ (Figs. 2, 3). Fourth, variations in the C/N ratio and the $\delta^{13}C_{org}$ could reveal lake level fluctuations, with higher C/N and $\delta^{13}C_{org}$ indicating a shallower lake with an expanded contribution of terrestrial and macrophyte-derived organic matter to the sediment[60]. However, within Zone 2, C/N values decrease and $\delta^{13}C_{org}$ increase, suggesting that the geochemical variations are not related to lake level fluctuations. Finally, declining C/N ratios with a corresponding rise in $\delta^{15}N_{org}$

could also be explained by greater delivery of nitrogen-rich and ^{15}N-enriched soil OM to the lake[45,46], as a consequence of soil erosion driven by fires and construction activities in the catchment.

However, a gradual but synchronous enrichment of $\delta^{15}N_{org}$ and $\delta^{13}C_{org}$, with a corresponding decline in the C/N ratio and an accompanied increase in $\delta^{13}C$ values for mid-chain *n*-alkanes (C_{25} and C_{27}; Fig. 2), suggest a progressive environmental change, which is most parsimoniously explained by environmental deterioration and aquatic macrophyte expansion in the lake. The gradual changes in bulk OM measurements ($\delta^{15}N_{org}$, $\delta^{13}C_{org}$, and C/N ratios) are inconsistent with the abrupt onset of both increased fire activity ca. 1070 BCE and enhanced clastic sedimentation related to the establishment of the urban grid ca. 710 BCE[8]. This suggests a progressive change in lake conditions rather than a shift in the source of terrestrial OM input (i.e., terrestrial vegetation, soil organics) to the lake. Furthermore, our interpretation for increased aquatic plant productivity is supported by similarities in organic matter proxies from Zone 2 with recent data, when the lake is known to have experienced eutrophication accompanied by macrophyte expansion[18–20] (Fig. S8).

Maximum lake disturbance conditions, inferred from increases in compound-specific $\delta^{13}C$, $\delta^{13}C_{org}$, $\delta^{15}N_{org}$, and a decline in C/N ratios, appear to have lasted about 350 years, from ~150 BCE to 200 CE, and coincided with the dense urban occupation at Nixtun-Ch'ich' and the enlargement of several monumental structures during the Late Preclassic[30]. Ecosystem alteration in the western arm of the lake was likely driven primarily by effluxes of soil phosphorus to the lake, first due to the removal of terrestrial vegetation that had previously anchored soil in the catchment and the use of slash-and-burn agricultural practices, and then as a result of construction events in the city and increased runoff via the streets[25]. Nutrient loading from fecal material derived from the peninsula, as evinced by a high average copro+epicopro concentration (Fig. 3), the highest cholestanol concentration ca. 250 BCE (95% range 565 BCE–85 CE), and elevated stigmastanol concentrations in the Late Preclassic (Fig. S4), may have also fueled primary productivity in the lake. Additional inputs of nutrients from human waste that accumulated in Preclassic ritual middens in Nixtun-Ch'ich' may have contributed to lake ecosystem alteration during the Late Preclassic but was likely not a dominant factor.

Previous studies of Petén lakes did not detect evidence of ancient, Maya-mediated deterioration of aquatic ecological conditions. Several factors may have facilitated aquatic ecosystem alteration at our study site: (1) shallow-water depths (8.4 m water depth at the coring site and generally less than 10 m in the area) in the western arm of Lake Petén Itzá, enabling high concentrations of nutrients in the water column; (2) poor hydrologic exchange of water between the narrow western arm and the rest of the lake (i.e., long water residence time and limited nutrient dilution); (3) proximity of Nixtun-Ch'ich' to the lake shore, which promoted drainage of nutrient-laden runoff from the city to the lake; (4) design of the streets, avenues, and canals in Nixtun-Ch'ich', which were paved with plaster and/or limestone flagstones[23–25] and likely expedited delivery of nutrient-rich runoff to the western arm of the lake; and (5) minimal presence of terrestrial, riparian vegetation to anchor surficial soils, as revealed by low abundances of charcoal beginning in the Middle Preclassic. Watershed deforestation is also supported by ref. [11], who attributed a shift to low fire activity ca. 450 BCE to earlier human-mediated forest reduction and consequent grassland expansion. In our sediment core collected near Nixtun-Ch'ich', however, low charcoal counts after ~710 BCE are likely the result of urbanization (i.e., heavy construction and occupation of Nixtun-Ch'ich'), which would have limited local forest recovery and enhanced nutrient delivery during dense Preclassic occupation of the city. Land clearance and urbanization limited fuel availability for fires and charcoal production and marked a human-induced shift from a high- to low-severity local fire regime on the Candelaria Peninsula.

Our sediment proxy reconstructions, when coupled with information from archeological excavations, shed light on the environmental consequences of ancient Maya settlement on lake ecological conditions. Archeological excavations at Nixtun-Ch'ich' show little evidence of Early Classic (250–600 CE) occupation[25], suggesting a population decline in the city during the Terminal Preclassic (ca. 100–250 CE). Archeological investigations have also found evidence for changes in Maya fishing practices at Nixtun-Ch'ich' during the Terminal Preclassic[61] that suggest that the Maya were catching smaller fish and hint at changing lake ecological conditions. Population decline and possible partial or temporary Late to Terminal Preclassic abandonment of the city coincides with ameliorating conditions in the lake after ~280 CE (95% range 45 BCE–560 CE). Rapid return of C/N, $\delta^{13}C_{org}$, and $\delta^{15}N_{org}$ to values similar to those in the lower part of the record (Fig. 2), combined with the statistical similarity of both $\delta^{13}C_{org}$ and C/N ratios in Zones 1 and 3 (Fig. 4), indicate that the western arm of Lake Petén Itzá recovered and reached stable limnological conditions by ca. 400 CE (95% range 90–640 CE). However, C/N ratios in Zone 3 were intermediate between Zones 1 and 2 (Fig. 4), suggesting that the extent of recovery was limited and did not fully return to its pre-disturbance state. Nevertheless, partial recovery occurred after the cessation of construction activities and dense human occupation. Consistent geochemical measures after ~400 CE, combined with persistent low charcoal abundance and stable magnetic stability and detrital elemental abundances (Fig. 3 and S7), indicate reduced Maya disturbance and decreased soil erosion, perhaps a result of the city's corridors having been plastered over during the Middle Preclassic period[25]. Occupation of Nixtun-Ch'ich' and its environs during the Classic and Postclassic periods[62], by dispersed, small settlements (of Chak'an Itzas during the Postclassic[63]) may have contributed to the limited recovery of the western arm of Lake Petén Itzá. Fluctuations in stigmastanol (Fig. S4) and low

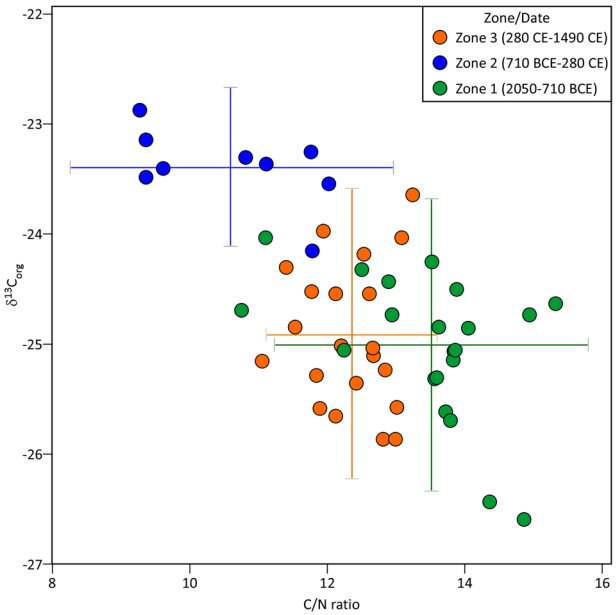

Fig. 4 Relationship between carbon to nitrogen ratios and organic carbon stable isotopes. Lake Petén Itzá C/N mass ratios and $\delta^{13}C_{org}$ by zone. Crosses indicate 2 standard deviation (2σ) ranges.

copro+epicopro concentrations (Fig. 3) suggest occasional pulses of herbivore[37,64] and human fecal material to the lake, potentially as a result of human presence at Nixtun-Ch'ich' during the Classic and Postclassic periods. Low copro+epicopro concentrations throughout most of the Classic and Postclassic periods also suggest that later populations were consistently small relative to Preclassic populations and that low-level Maya occupation of Nixtun-Ch'ich' prevented full recovery of the lake to pre-disturbance conditions, after almost 1000 years of environmental degradation.

Methods

In July 2018, we collected two sediment cores from Lake Petén Itzá, in the vicinity of the southern lowland Maya site of Nixtun-Ch'ich'. Here, we report the findings from one of the cores (PI-NC-1) and expand upon the findings by Obrist-Farner and Rice[8].

Core collection. The 515-cm-long sediment core (PI-NC-1) was collected ~200 m south of the Maya archeological site of Nixtun-Ch'ich' (16°56'36" N, 89°55'56" W), in the narrow, western arm (7 km long and 250–450 m wide) of the southern basin of the lake (Fig. 1). The location is downgradient from Avenues G and H in the city (Fig. 1), which run adjacent to major structures in Nixtun-Ch'ich' and carried runoff from the site into the lake. The core was collected in 8.4 m of water from a wooden platform mounted on two *lanchas* (motorized canoes). The 72-cm mud-water interface (MWI) core was collected using a modified piston corer designed to obtain undisturbed MWI sediments[65]. The unconsolidated MWI sediments were extruded vertically in the field, sectioned at 2.0-cm intervals, and placed into labeled Whirl-Pak^{TM} bags. Next, six sequential sections of core were collected from 50 to 515 cm depth using a modified Livingstone-type piston corer designed for the collection of deeper, consolidated deposits. These core sections were kept in labeled polycarbonate tubes that were wrapped in plastic. After collection, the core material was transported to the laboratory for further analysis.

Age-depth modeling. We refined the existing age-depth model for the PI-NC-1 core that was presented by ref. [8] and used six radiocarbon dates. This study used six additional samples of terrestrial wood charcoal (Supplementary Data 1). Three of the new charcoal samples were out of stratigraphic order and discarded. For radiocarbon analysis, all charcoal samples were washed with deionized water over a 125-µm sieve to remove adhering sediment, wrapped in aluminum foil, and submitted to the Center for Accelerator Mass Spectrometry at Lawrence Livermore National Laboratory. We created a new age-depth model (Figs. S1, S2) by applying the Bayesian software Bacon (rbacon package in R[66]) calibrated with IntCal20[67], and the date the core was collected (2018). All dates came from terrestrial wood (charcoal) to avoid potential effects from "hard-water-lake error," which may confound dates on bulk organic matter in this limestone bedrock region[3]. We report mean date estimates from the age-depth model to characterize the timing of changes detected in the core. The timing of the Maya clay is constrained by a radiocarbon age 9 cm below and 21 cm above the massive deposits, resulting in a sedimentation rate of ~0.15 cm/yr (Fig. S2). Several previous investigations in Lake Petén Itzá[3,5,7,11] also report a similar sedimentation rate during Preclassic and Classic Maya times based on radiocarbon age-depth models, supporting our Bayesian modeling results.

Geochemical analysis. Samples for geochemical analyses were collected at 5-cm intervals along the length of the core, from 313 to 53 cm depth. Samples from the uppermost 50 cm, from the MWI core, were collected at intervals of 4 or 6 cm. Samples were oven-dried at 60 °C for 15 h, ground to a fine powder with a ceramic mortar and pestle, and placed into labeled 20-mL scintillation vials. Total carbon (TC) and total nitrogen (TN) were measured using a Carlo Erba NA 1500 CNS elemental analyzer. Total inorganic carbon (TIC) was determined by coulometric titration using an AutoMate^{TM} acidification preparation device coupled with a UIC^{TM} 5017 CO_2 coulometer. Total organic carbon (TOC) was calculated as TC minus TIC. TOC/TN mass ratios (i.e., C/N ratios) were computed by dividing TOC (wt %) by TN (wt %). Samples for bulk carbon stable isotope ($\delta^{13}C_{org}$) analysis were treated with 1 N HCl to remove carbonate and then washed with distilled water to remove chloride. Samples for nitrogen stable isotope ($\delta^{15}N_{org}$) analysis of bulk organic matter were not acidified. Samples were loaded into tin capsules and placed in a 50-position automated carrousel on a Carlo Erba NA 1500 elemental analyzer. After combustion at 1020 °C, gases were carried in a helium stream through a Conflo II interface to a Thermo Electron Delta V Advantage isotope ratio mass spectrometer (IRMS) to measure the carbon and nitrogen stable isotope compositions of bulk organic matter. Carbon isotope results are expressed as per mil (‰) in standard delta notation relative to Vienna Pee Dee Belemnite (VPDB). Nitrogen isotope results are expressed as the per mil (‰) deviation from atmospheric nitrogen (AIR, $\delta^{15}N_{org} = 0$). We also calculated the mean and 2 standard deviations (2σ) ranges of C/N mass ratios and $\delta^{13}C_{org}$ for each zone (Figs. 4, S5, and Supplementary Data 2) to determine whether the values reflect statistically similar or different lake conditions in each zone. All zonal averages are reported with standard deviation values.

***n*-Alkane quantification and isotope analysis**. For *n*-alkane quantification, 38 samples were collected across 2-cm intervals from 13 cm to 310 cm core depth. Freeze-dried and homogenized samples (2.05–8.95 g) were extracted using an accelerated solvent extractor (ASE) with 9:1 (*v*:*v*) dichloromethane:methanol (DCM:MeOH). The total lipid extract (TLE) was then separated using a deactivated alumina oxide column to isolate the apolar fraction containing the *n*-alkanes using 9:1 hexane:DCM solution and purified using Ag^+ impregnated silica gel column chromatography and hexane eluant to isolate the saturated hydrocarbons. Samples were spiked with 50 ng/µL 5α-Androstane standard and analyzed using a Thermo Trace Ultra ISQ gas chromatograph (GC) with a mass spectrometer (MS) and a flame ionization detector (FID) to identify and quantify the *n*-alkanes, respectively. Samples were injected at 300 °C with a 30-m fused silica column (DB-5, 0.25 mm ID, 0.25 µm film thickness) using hydrogen as the carrier gas. Following a 1-min hold at 80 °C, the GC oven temperature was ramped to 320 °C at a rate of 13 °C/min, with a final hold of 20 min. The *n*-alkanes were identified by retention times of a standard *n*-alkane mix and through a comparison of fragmentation patterns in an MS library. Quantification of *n*-alkanes was ascertained via comparison of GC-FID sample peak integration to the standard, and total *n*-alkane abundance is expressed as the summed absolute concentration of C_{16} to C_{35} relative to dry sediment weight (µg/g dry sediment). Compound-specific carbon stable isotopes for select *n*-alkanes (C_{23}–C_{35}) were determined by GC-combustion (C)-IRMS. GC-C-IRMS analyses were performed with a Trace 1310 GC coupled to a Finnigan Delta V Plus IRMS via a Thermo GC-Isolink at McGill University. Samples were injected at 300 °C with a 60-m fused silica column (Thermo TR-5, 0.25 mm ID, 0.25 µm film thickness) using helium as the carrier gas. We used an oven program of 60 °C isothermal (1 min), ramp to 320 °C at 5 °C/min, and a 320 °C isothermal (10 min). Carbon isotope values of samples are reported in delta notation relative to the standard VPDB. *n*-Alkane carbon isotope ratios were normalized to the VPDB scale using a linear calibration of *n*-alkane primary reference materials (Mix A6, Arndt Schimmelmann, Indiana University), analyzed at the beginning, middle, and end of each sequence, with an overall precision of 0.35‰. Accuracy and precision were also monitored with measurements of an internal laboratory standard produced from extracts of maple leaves that was analyzed after every third sample. The standard deviation of the laboratory standard ($n = 28$) was 0.4‰ over the duration of the analysis. Sample standard errors were calculated using the method adapted for $\delta^{13}C$ measurements[68], which accounts for sample reproducibility and errors in VPDB scale normalization, and ranged between 0.22 to 0.26‰. All zonal averages are reported with standard deviation values.

Fecal sterol analysis. For fecal stanol/sterol quantification, 59 samples were collected along the length of the 515-cm core. Samples were analyzed using the previously reported protocol of ref. [39]. In summary, samples were freeze-dried, homogenized, and weighed. Then, sediment samples were placed in PTFE tubes and extracted using a CEM MARS 6 microwave extractor heated at 80 °C for 20 min with 10 mL of 9:1 DCM:MeOH solution. The contents of the PTFE tubes were then transferred to centrifuge vials and centrifuged to obtain the TLE. Next, each TLE was run through a chromatographic column containing 5 cm of sodium sulfate to remove water. The TLE was then saponified using KOH and the neutral fraction containing sterols was extracted three times using liquid-liquid extractions with 10 mL of 2:1 hexane:dichloromethane solution. The neutral fraction was then fully evaporated and derivatized with 200 µL each of BSTFA (bis-trimethylsilyl trifluoroacetamide) and pyridine to replace the hydrogen with the less exchangeable trimethylsilyl (TMS) group. The neutral (sterol) fraction was analyzed using gas chromatography with a flame ionization detector (GC-FID) with a TRACE TR-5 GC Column (60 m × 0.25 mm) in sequence with known standards for cholestanol, cholesterol, stigmastanol, coprostanol, and epicoprostanol (Sigma-Aldrich) in order to quantify the compounds as compared to the standards via peak integration. A standard volume of sample was injected (1 µL) for each quantification. A set of ten representative samples were analyzed using an Agilent 7890B GC with an Agilent 5977B MSD (DB-5MS 25 m × 200 µm × 0.33 µm) at Concordia University to confirm compound identification. Fecal stanol/sterol concentrations include all isomers of the compounds and are expressed as absolute concentrations relative to dry sediment weight (µg/g dry sediment) and normalized to TOC (µg/g of OC). For interpretation of stanol/sterol abundances, we focus on concentrations normalized to TOC to account for the effects of mineral dilution, as well as the potential effects of organic matter deposition and preservation on stanol/sterol concentrations[69,70]. We report the sum of epicoprostanol and coprostanol (after ref. [71] and ref. [39]) because it was not possible to consistently resolve these molecules due to their overlapping retention times. Epicoprostanol is a transformation product of coprostanol in the environment[72], and therefore their summed concentration represents the net input of coprostanol to lake sediments. All zonal averages are reported with standard deviation values.

Charcoal analysis. Charcoal analyses were carried out following the macroscopic sieve procedure of the National Lacustrine Core Facility (LacCore) at the University of Minnesota, outlined below. For the analyses, ~1 cm^3 of the wet sample

was collected from 2-cm core depth intervals in MWI sediments and 1-cm core depth intervals from depths of 50 to 313 cm. Samples were first treated with ~25 mL hydrogen peroxide (6%), covered with aluminum foil, and heated at ~50 °C for 24 h to oxidize organic matter. Next, each sample was washed gently over a 125-µm sieve, and the retained fraction was collected into a 100 mm × 15 mm polystyrene petri dish. Charcoal particles >125 µm are likely to have been derived from local, rather than distant, fires, thus representing the fire history in the immediate vicinity of the core location[73]. Next, ~15 mL hydrogen peroxide (6%) was added to the petri dish and the sample was covered with aluminum foil and allowed to dry for 24–72 h at ~50 °C. After drying, macroscopic charcoal particles were counted under a Leica S9i microscope at 25x magnification. All zonal averages are reported with standard deviation values.

Data availability

Data for replicating the results of this study are available as supplementary files. All geochemical data and radiocarbon dates have been uploaded to the NCEI NOAA repository[74] and can be found at https://www.ncei.noaa.gov/access/paleo-search/study/37383.

Received: 24 June 2022; Accepted: 22 February 2023;
Published online: 04 March 2023

References

1. Deevey, E. S. et al. Mayan urbanism: Impact on a tropical karst environment. *Science* **206**, 298–306 (1979).
2. Islebe, G. A., Hooghiemstra, H., Brenner, M., Curtis, J. H. & Hodell, D. A. A Holocene vegetation history from lowland Guatemala. *Holocene* **6**, 265–271 (1996).
3. Curtis, J. H. et al. A multi-proxy study of Holocene environmental change in the Maya Lowlands of Peten, Guatemala. *J. Paleolimnol.* **19**, 139–159 (1998).
4. Leyden, B. W., Brenner, M. & Dahlin, B. H. Cultural and climatic history of Cobá, a lowland Maya city in Quintana Roo, Mexico. *Quat. Res.* **49**, 111–122 (1998).
5. Rosenmeier, M. F., Hodell, D. A., Brenner, M., Curtis, J. H. & Guilderson, T. P. A 4000-year lacustrine record of environmental change in the southern Maya lowlands, Petén, Guatemala. *Quat. Res.* **57**, 183–190 (2002).
6. Wahl, D., Estrada-Belli, F. & Adnerson, L. A 3400 year paleolimnological record of prehispanic human–environment interactions in the Holmul region of the southern Maya lowlands. *Palaeogeogr. Palaeoclimatol. Palaeoecol.* **379-380**, 17–31 (2013).
7. Battistel, D. et al. Anthropogenic impact in the Maya lowlands of Petén, Guatemala, during the last 5500 years. *J. Quat. Sci.* **33**, 166–176 (2018).
8. Obrist-Farner, J. & Rice, P. M. Nixtun-Ch'ich' and its environmental impact: Sedimentological and archaeological correlates in a core from Lake Petén Itzá in the southern Maya lowlands, Guatemala. *J. Archaeol. Sci. Rep.* **26**, 101868 (2019).
9. Anselmetti, F. S., Hodell, D. A., Ariztegui, M., Brenner, M. & Rosenmeier, M. F. Quantification of soil erosion rates related to ancient Maya deforestation. *Geology* **35**, 915–918 (2007).
10. Mueller, A. D. et al. Climate drying and associated forest decline in the lowlands of northern Guatemala during the late Holocene. *Quat. Res.* **71**, 133–141 (2009).
11. Schüpbach, S. et al. Combining charcoal sediment and molecular markers to infer a Holocene fire history in the Maya Lowlands of Petén, Guatemala. *Quat. Sci. Rev.* **115**, 123–131 (2015).
12. Beach, T. et al. Ancient Maya impacts on the Earth's surface: an early anthropocene analog? *Quat. Sci. Rev.* **124**, 1–30 (2015).
13. Beach, T. et al. Ancient Maya wetland fields revealed under tropical forest canopy from laser scanning and multiproxy evidence. *Proc. Natl. Acad. Sci. USA* **116**, 21469–21477 (2019).
14. Krause, S. et al. Tropical wetland persistence through the Anthropocene: multiproxy reconstruction of environmental change in a Maya agroecosystem. *Anthropocene* **34**, 100284 (2021).
15. Rice, P. M. & Rice, D. S. in *Historical and Archaeological Perspectives on the Itzas of Petén, Guatemala* (eds Rice, P. M. & Rice, D.S.) Ch. 1 (University Press of Colorado, 2018).
16. Deevey, E. S. Stress, strain and stability in lacustrine ecosystems, in *Lake Sediments and Environmental History* (eds Haworth, E. Y. & Lund, J. W. G) 203–229 (Leicester: Leicester University Press, 1984).
17. Brenner, M., Rosenmeier, M. F., Hodell, D. A. & Curtis, J. H. Paleolimnology of the Maya lowlands: long-term perspectives on interactions among climate, environment, and humans. *Ancient. Mesoamer.* **13**, 141–157 (2002).
18. Rosenmeier, M., Brenner, M., Kenney, W. F., Whitmore, T. J. & Taylor, C. M. Recent eutrophication in the southern basin of Lake Petén Itzá, Guatemala: human impact on a large tropical lake. *Hydrobiologia* **511**, 161–172 (2004).
19. Pérez, L. et al. Post-Columbian environmental history of Lago Petén Itzá, Guatemala. *Rev. Mex. Cienc. Geo.* **27**, 490–507 (2010).
20. Reyes Morales, E. M. *Los cuerpos de agua de la region Maya Tikal-Yaxhá: Importancia de la vegetación acuática asociada, su conservación y el valor desde el uso humano* (Secretaria Nacional de Ciencias y Tecnología, 2008).
21. Obrist-Farner, J., Brenner, M., Curtis, J. H., Kenney, W. F. & Salvinelli, C. Recent onset of eutrophication in Lake Izabal, the largest water body in Guatemala. *J. Paleolimnol.* **62**, 359–372 (2019).
22. Waters, M. N. et al. Harmful algal blooms and cyanotoxins in Lake Amatitlán, Guatemala, coincided with ancient Maya occupation in the watershed. *Proc. Natl. Acad. Sci. USA* **118**, e2109919118 (2021).
23. Rice, P. M. & Pugh, T. W. Middle preclassic Nixtun-Ch'ich': a lowland Maya primate/ritual city. *J. Anthrop. Archaeol.* **63**, 101308 (2021).
24. Pugh, T. W., Rice, P. M., Chan Nieto, E. M., Meranda, M. L. & Milley, D. S. Middle preclassic hydraulic planning at Nixtun-Ch'ich', Petén, Guatemala. *Ancient Mesoamer* **33**, 589–603 (2022).
25. Pugh, T. W. & Rice, P. M. Early urban planning, spatial strategies, and the Maya gridded city of Nixtun-Ch'ich', Petén, Guatemala. *Curr. Anthropol.* **58**, 576–603 (2017).
26. Vinson, G. L. Upper cretaceous and tertiary stratigraphy of Guatemala. *AAPG Bull* **46**, 425–456 (1962).
27. Hodell, D. A., Quinn, R. L., Brenner, M. & Kamenov, G. Spatial variation of strontium isotopes ($^{87}Sr/^{86}Sr$) in the Maya region: a tool for tracking ancient human migration. *J. Archaeol. Sci.* **31**, 585–601 (2004).
28. Anselmetti, F. S. et al. Late Quaternary climate-induced lake level variations in Lake Petén Itzá, Guatemala, inferred from seismic stratigraphic analysis. *Palaeogeogr. Palaeoclimatol. Palaeoecol.* **230**, 52–69 (2006).
29. Brenner, M. in *Historical and Archaeological Perspectives on the Itzas of Petén Guatemala* (eds Rice, P. M. & Rice, D. S.) Ch. 3 (University Press of Colorado, 2018).
30. Pugh, T. W. From the streets: public and private space in an early Maya city. *J. Archaeo. Method Theory* **26**, 967–997 (2019).
31. Rice, P. M. Early pottery and construction at Nixtun-Ch'ich', Petén, Guatemala: preliminary observations. *Latin. Amer. Antiq.* **30**, 471–489 (2019).
32. Dunning, N. P., Beach, T. P. & Luzzadder-Beach, S. Kax and kol: collapse and resilience in lowland Maya civilization. *Proc. Natl. Acad. Sci. USA* **109**, 3652–3657 (2012).
33. Jones, G. D. *The Conquest of the Last Maya Kingdom* (Stanford Univ. Press, 1998).
34. Rice, P. M. Mound ZZI, Nixtun-Ch'ich', Petén, Guatemala: rescue operations at a long-lived structure in the Maya lowlands. *J. Field. Archaeol.* **34**, 403–422 (2009).
35. Meyers, P. A. & Teranes, J. L. in *Tracking Environmental Change Using Lake Sediments: Physical and Geochemical Methods* (eds Last, W. M. & Smol, J. P.) Ch. 9 (Springer, 2001).
36. Fellerhoff, C., Voss, M. & Wantzen, K. M. Stable carbon and nitrogen isotope signatures of decomposing tropical macrophytes. *Aquat. Ecol.* **37**, 361–375 (2003).
37. Prost, K., Birk, J. J., Lehndorff, E., Gerlach, R. & Amelung, W. Steroid biomarkers revisited – Improved source identification of faecal remains in archaeological soil material. *PLoS ONE* **12**, e0164882 (2017).
38. Zocatelli, R. et al. Fecal biomarker imprints as indicators of past human land uses: Source distinction and preservation potential in archaeological and natural archives. *J. Archaeol. Sci.* **81**, 79–89 (2017).
39. Keenan, B. et al. Molecular evidence for human population change associated with climate events in the Maya lowlands. *Quat. Sci. Rev.* **258**, 106904 (2021).
40. Fan, J. et al. Carbon and nitrogen signatures of sedimentary organic matter from Dali Lake in Inner Mongolia: implications for Holocene hydrological and ecological variations in the East Asian summer monsoon margin. *Quat. Int.* **452**, 65–78 (2017).
41. Fisher, E. et al. Molecular marker records of land use change. *Org. Geochem.* **34**, 105–119 (2003).
42. Enters, D., Lücke, A. & Zolitschka, B. Effects of land-use change on deposition and composition of organic matter in Frickenhauser Sea, northern Bavaria, Germany. *Sci. Total Environ.* **369**, 178–187 (2006).
43. Inglett, P. W. & Reddy, K. R. Investigating the use of macrophyte stable C and N isotopic ratios as indicators of wetland eutrophication: patterns in the P-affected Everglades. *Limnol. Oceanogr.* **51**, 2380–2387 (2006).
44. Aichmer, B., Herzschuh, U. & Wilkes, H. Influence of aquatic macrophytes on the stable carbon isotopic signatures of sedimentary organic matter in lakes on the Tibetan Plateau. *Org. Geochem.* **41**, 706–718 (2010).
45. Talbot, M. R. in *Tracking Environmental Change Using Lake Sediments: Physical and Geochemical Methods* (eds Last, W. M. & Smol, J. P) Ch. 15 (Kluwer Academic Publishers, 2001).

46. Lou, Y., Xu, M., Chen, X., He, X. & Zhao, K. Stratification of soil organic C, N and C:N ratio as affected by conservation tillage in two maize fields of China. *CATENA* **95**, 124–130 (2012).
47. Hollander, D. J. & McKenzie, J. A. CO_2 control on carbon-isotope fractionation during aqueous photosynthesis: a paleo-pCO_2 barometer. *Geology* **19**, 929–932 (1991).
48. Gong, X. et al. Spatial patterns of leaf $\delta^{13}C$ and $\delta^{15}N$ of aquatic macrophytes in the arid zone of northwestern China. *Ecol. Evol.* **11**, 3110–3119 (2021).
49. Berke, M. A. in *Methods in Paleoecology: Reconstructing Cenozoic Terrestrial Environments and Ecological Communities* (eds Croft, D. A., Su, D. F. & Simpson, S. W.) Ch. 8 (Springer, 2018).
50. Douglas, P. M. J., Pagani, M., Brenner, M., Hodell, D. A. & Curtis, J. H. Aridity and vegetation composition are important determinants of leaf-wax δD values in southeastern Mexico and Central America. *Geochim. Cosmochim. Acta* **97**, 24–45 (2012).
51. Cranwell, P. A., Eglinton, G. & Robinson, N. Lipids of aquatic organisms as potential contributors to lacustrine sediments—II. *Org. Geochem.* **11**, 513–527 (1987).
52. Mays, J. L. et al. Stable carbon isotopes ($\delta^{13}C$) of total organic carbon and long-chain *n*-alkanes as proxies for climate and environmental change in a sediment core from Lake Petén-Itzá, Guatemala. *J. Paleolimnol.* **57**, 307–319 (2017).
53. Ficken, K. J., Li, B., Swain, D. L. & Eglinton, G. An n-alkane proxy for the sedimentary input of submerged/floating freshwater aquatic macrophytes. *Org. Geochem.* **31**, 745–749 (2000).
54. He, D. et al. Distribution of n-alkanes and their δ^2H and $\delta^{13}C$ values in typical plants along a terrestrial-coastal-oceanic gradient. *Geochim. Cosmochim. Acta* **281**, 31–52 (2020).
55. Huang, Y. et al. Climate change as the dominant control on glacial-interglacial variations in C_3 and C_4 plant abundance. *Science* **293**, 1647–1651 (2001).
56. Wright, D. K. et al. Iron age landscape changes in the Benoué River Valley, Cameroon. *Quat. Res.* **92**, 323–339 (2019).
57. Lichtfouse, É., Elbisser, B., Balesdent, J., Mariotti, A. & Bardoux, G. Isotope and molecular evidence for direct input of maize leaf wax n-alkanes into crop soils. *Org. Geochem.* **22**, 349–351 (1994).
58. Miller, S. S., Redi, L. M., Butler, G., Winter, S. P. & McGoldrick, N. J. Long chain alkanes in silk extracts of maize genotypes with varying resistance to fusarium graminearum. *J. Agric. Food. Chem.* **51**, 6702–6708 (2003).
59. Mueller, A. D. et al. Recovery of the forest ecosystem in the tropical lowlands of northern Guatemala after disintegration of Classic Maya polities. *Geology* **38**, 523–526 (2010).
60. Haberzettl, T. et al. Climatically induced lake level changes during the last two millennia as reflected in sediments of Laguna Potrok Aike, southern Patagonia (Santa Cruz, Argentina). *J. Paleolimnol.* **33**, 283–302 (2005).
61. Rice, P. M. & Rice, D. S. *Small Things Forgotten: Artifacts of Fishing in the Petén Lakes Region, Guatemala* (Society of Ethnobiology, 2017).
62. Rice, P. M. Wanna Bet? Classic ballcourt 2 at Nixtun-Ch'ich', Peten, Guatemala. *Latin. Amer. Antiq.* **29**, 610–615 (2018).
63. Pugh, T. W., Rice, P. M., Nieto, E. C. & Rice, D. S. A Chak'an Itza Center at Nixtun-Ch'ich', Petén, Guatemala. *J. Field. Archaeol.* **41**, 1–16 (2016).
64. Sharpe, A. E. et al. Earliest isotopic evidence in the Maya region for animal management and long-distance trade at the site of Ceibal, Guatemala. *Proc. Natl. Acad. Sci. USA* **115**, 3605–3610 (2018).
65. Fisher, M. M., Brenner, M. & Reddy, K. R. A simple, inexpensive piston corer for collecting undisturbed sediment/water interface profiles. *J. Paleolimnol.* **7**, 157–161 (1992).
66. Blaauw, M. & Christe, J. A. Flexible paleoclimate age-depth models using an autoregressive gamma process. *Bayesian Anal.* **6**, 457–474 (2011).
67. Reimer, P. J. et al. The IntCal20 northern hemisphere radiocarbon age calibration curve (0–55 cal kBP). *Radiocarbon* **62**, 725–757 (2020).
68. Polissar, P. & D'Andrea, W. Uncertainty in paleohydrologic reconstructions from molecular δD values. *Geochim. Cosmochim. Acta* **129**, 146–156 (2014).
69. LeBlanc, L. A., Latimer, J. S., Ellis, J. T. & Quinn, J. G. The geochemistry of coprostanol in waters and surface sediments from Narragansett Bay. *Estuar. Coast. Shelf Sci.* **34**, 439–458 (1992).
70. Thienemann, M. et al. Organic geochemical and palynological evidence for Holocene natural and anthropogenic environmental change at Lake Dojran (Macedonia/Greece). *Holocene* **27**, 1103–1114 (2017).
71. White, A. J. et al. An evaluation of fecal stanols as indicators of population change at Cahokia, Illinois. *J. Archaeol. Sci.* **93**, 129–134 (2018).
72. Bull, I. D., Lockheart, M. J., Elhmmali, M. M., Roberts, D. J. & Evershed, R. P. The origin of faeces by means of biomarker detection. *Environ. Int.* **27**, 647–654 (2002).
73. Whitlock, C. & Larsen, C. in *Tracking Environmental Change Using Lake Sediments: Terrestrial, Algal, and Siliceous Indicators* (eds Smol, J. P., Birks, H. J. B. & Last, W. M.) Ch. 5 (Kluwer Academic Publishers, 2001).
74. Birkett, B. et al. Degradation of Lake Petén Itzá, Guatemala, National Centers for Environmental Information (NCEI) Dataset. https://www.ncei.noaa.gov/access/paleo-search/study/37383 (2023).

Acknowledgements

This work was partially supported by NSF/GSA (National Science Foundation/Geological Society of America) Graduate Student Geoscience Grant # 13171-21, which is funded by NSF Award # 1949901. This research was also partially supported by a Society for Sedimentary Geology (SEPM) Student Research Grant, the Dr. Alfred Spreng Graduate Research Award (Missouri University of Science and Technology), and an NSF-EAR Postdoctoral Research Fellowship to WGP. We thank Evelyn Chan for arranging the construction of the coring platform in Petén and the Guatemalan Instituto de Antropología e Historia (IDEAH) for permission to export the cores. We also thank Defensores de la Naturaleza and the Consejo Nacional de Áreas Protegidas (CONAP) for providing personnel to help with coring. We would also thank E. Duarte for assistance with age-depth modeling and charcoal analysis, P. Cho for assistance with *n*-alkane quantifications, T.H. Bui for assistance with *n*-alkane $\delta^{13}C$ measurements, and A. Hoffmann for general laboratory assistance. We also thank M. Brenner for insightful discussions and for his thoughtful review of an earlier version of this manuscript, and we thank J. Maurer, D. Wronkiewicz, and D. Borrok for insightful discussions.

Author contributions

B.A.B., J.O.-F., and P.M.R. conceptualized this study. B.A.B., W.G.P., P.M.J.D., M.A.B., A.K.T., J.H.C., and B.K. helped with the geochemical analysis. The original draft was put together by B.A.B. and J.O.F. P.M.R., P.M.J.D., M.A.B., and J.H.C. contributed to reviewing and editing the manuscript.

Competing interests

The authors declare no competing interests.

Additional information

Supplementary information The online version contains supplementary material available at https://doi.org/10.1038/s43247-023-00726-4.

Correspondence and requests for materials should be addressed to Jonathan Obrist-Farner.

Peer review information *Communications Earth & Environment* thanks the anonymous reviewers for their contribution to the peer review of this work. Primary Handling Editors: Olga Churakova and Joe Aslin. Peer reviewer reports are available.

Reprints and permission information is available at http://www.nature.com/reprints

Publisher's note Springer Nature remains neutral with regard to jurisdictional claims in published maps and institutional affiliations.